

Effect of Permeability and Geomechanical Properties on Coal Matrix During CBM Production – An Overview

Harinandan Kumar^{1*}, M.K. Mishra¹ and S. Mishra²

¹Department of Mining Engineering N.I.T., Rourkela, 769008, India

²Department Chemical Engineering N.I.T., Rourkela, 769008, India

Received 15 October 2017; Accepted 10 February 2018

Abstract

This review presents a comprehensive overview of the technologies and engineering of permeability behaviour of coal matrix as well as impact of induced stress-strain during CBM production. It emphasizes on the transport of gas in coal matrix as well as behaviour of coal matrix towards permeability conditions during adsorption/desorption processes. The impacts of stress- strain on permeability of coal matrix are also discussed. The effect on permeability of coal matrix and its shrinkage/swelling during adsorption/desorption of gases has been deliberated. The pore pressure and permeability of cleat structure that regulates the production of coal bed methane was reflected. In this paper the overview of coal bed methane generation and production, gas transport in coal matrix, changes in coal matrix during adsorption/desorption process, permeability behaviour of coal matrix and impact of spatial stress-strain on coal matrix were studied.

Keywords: Coal Bed Methane, Transport of gas, Coal Matrix, Permeability, Geo-mechanical Properties

1. Introduction

Successful production of coal bed methane and sequestration of carbon dioxide in coal seams requires knowledge of coal structural properties and their variation under in situ conditions. Coals, irrespective of their rank, macerals composition and nature of occurrence, retain large amounts of mixture of gases (methane and other gases) within it. The extraction of coal bed methane is well established and establishing in some of the developed as well as developing countries like USA, Australia, China, India and Canada etc. It was observed that coal bed methane is formed under coalification process either by biogenic or thermogenic degradation of buried plant materials [1]. Biogenic conversion of plant materials into methane occurs due to microbial action [2, 3] while thermogenic conversion/thermal decarboxylation is due to high temperature and pressure [4]. Thermogenic conversion of plant materials is the chemical process which converts the vegetal remains into CH₄. Methane is found adsorbed in internal surface of coal matrix and hence amount of methane in coal matrix depend on the pore surface area of matrix [5-7]. Pores of coal matrix mainly divided into macro pores (> 50 nm), meso pores (between 2 and 50 nm) and micro pores (< 2 nm) [8, 9]. Micro pores consist of majority of methane gas in coal matrix while probability of finding methane gas in meso and macro pores is less [8, 9]. It is estimated that majority of the methane is typically adsorbed in the micro pores and very little resides in the macro pores [10]. The gas content in coal bed is determined by presence of macerals in coal. The major macerals presents in coal are Vitrinite,

Liptinite and Inertinite [11]. Weishauptova et al., 2014 [12] observed that the sorption capacity of the organic matter in a coal sample with a prevalence of inertinite (63.0%) was lower than in a sample with a prevalence of vitrinite (65.3%) by only 14% for CO₂ and by 18% for CH₄. Moore, 2012 [13] observed that the organic composition of coal holds principal role in determination of porosity and permeability character and maximum gas holding capacity. The low pressure in coal reservoir in CBM production cause matrix shrinkage that enlarges cleat aperture and as a result micro cleats opens to enhance gas permeability [14-16]. Cleat structure plays leading role for the flow of methane in coal matrix. Flow of gases in coal bed is usually dendritic in nature i.e. migration of gas takes place from small pores (micro cleats) to medium pores (meso cleats) and then moves to large pores (macro cleats) respectively. Characterisation of CBM in coal matrix is a challenge to determine the permeability and percentage gas saturation. Permeability gives the general outlook of flow behaviour of gases in coal matrix. Percentage of gas saturation, gas rate and recoverability of gas from a reservoir mainly determined by adsorption/desorption behaviour of coal matrix [17-19]. These parameters are highly applicable during the modelling of gas flow behaviour in reservoir. Designing a successful pilot well programme as well as production wells depends on the permeability and percentage gas saturation character in coal matrix [13]. The approach taken in this review aims to satisfy a deceptive need for a current and brief summary of permeability, flow behaviour and geo-mechanical properties of coal matrix. Statistics of coal and coal bed methane across the globe is shown in (Table 1, 2 and Figure 1).

Methane is always hazardous in underground mining. The ventilation system is generally provided to combat accidental explosion of methane gas, and release of methane

*E-mail address: harinandankumar88@gmail.com

ISSN: 1791-2377 © 2018 Eastern Macedonia and Thrace Institute of Technology. All rights reserved.

doi:10.25103/jestr.112.22

in atmosphere. Venting of methane in atmosphere not only cause greenhouse effect but also loss of clean fuel. Modern development and engineering technology in extraction method made the production of coal bed methane practical and feasible. The attempts to isolate and pipe gas from a coal mine were occurred in Great Britain in 1733. The first recorded successful use of a vertical borehole to drain gas from virgin coal was occurred in the Mansfield Colliery (Ruhr, Germany) in 1943. The first serious research concerning coal bed methane production in the United States occurred in the 1970s with a test project in the Black Warrior basin in Alabama. In the 1980s the Gas Research Institute began its coal bed methane explores. Their activities dealt with cooperative well studies, reservoir engineering analysis, fracturing and completion work as well as operational improvements and recompletion of wells. An indicator for coal bed methane has emerged as a valuable energy resource is the increased production of CBM in the Appalachian, Black Warrior, San Juan, Piceance, Powder River and Greater Green River Basins. Coal bed methane (CBM) also known as coal seam gas (CSG) is simply methane (CH₄) gas found adsorbed in coal seam. CBM is similar to natural gas which contains about 95% of pure methane [22]. CBM doesn't contain hydrogen sulphides as compared to oil, coal or even conventional natural gas so it is more environmentally friendly hence named as "Sweet Gas". Trace amount of propane/butane and almost negligible amount of natural gas condensate are found in CBM [23]. Methane is mostly found adsorbed in coal matrix. Cleat structure in coal matrix is the path way for migration of methane from coal to atmosphere. Methane present in macro cleat migrates to atmosphere while methane present in micro cleat remains adsorbed on internal surface of coal matrix. CBM serves both the source rock as well as the reservoir rock hence it is considered as non-conventional source [24]. Storage and migration of methane in coal matrix is comparatively complex. There are following ways of storage of coal bed methane in coal seam (Figure 2):

Table 1. Coal resources and CBM across the world [20]

SI. NO.	Country	Coal resources (BT)	CBM resource (TCM)
1	Canada	7,000	6.5-76.4
2	Russia	6,500	13.3-73.6
3	China	4,000	16.4-34.0
4	US	3,970	12.7-25.5
5	Australia	1,700	8.8-14.2
6	India	522	1.4-2.6
7	Germany	320	1.7-2.5
8	U.K.	190	1.1-1.7
9	Poland	160	1.4-2.0
10	South Africa	150	1.4-2.0
11	Indonesia	17	0.1-0.2
12	Zimbabwe	8	0.04-0.05

Commercial grade of coal for CBM should have at least 8.5 cc/gm of methane [26]. Study shows 11.50, 12.30 and 5.40 cc/gm CBM potentialities in Korba, Ib and Umaria valley seams [27]. Chatterjee and Paul, 2013 [28] determined gas content of various seams in central Jharia, India and found to vary between 11.11 cc/g and 11.91 cc/g. It was estimated that, the coal reservoir possesses a high gas content, high permeability, and high gas production for a depth between 400 to 700m [25, 29-30]. At the depth more

than 700m, the gas content as well as gas production decreases, which reflect that, the CBM enrichment and development conditions deteriorate [29]. The main parameters affecting the coal-bed gas enrichment area are the burial depth, the gas content, the individual coal bed layer thickness, the overall structure thickness, and the abundance of the resource. The geological factors affecting these parameters are the sedimentary environment and the structural evolution in the region, and the geo-hydrologic conditions [31, 32]. Statistics of coal reservoir properties of worldwide and India is shown in (Table 3, 4 and 5).

Table 2. Established CBM reserve in India [20]

SI. No.	Block Name	Operator	Reserve Established (TCF)
1	SP(East)-CBM-2001/I	RIL	1.69
2	SP(WEST)-CBM-2001/I	RIL	1.96
3	Raniganj (South)	GEECL	1.385
4	BK-CBM-2001/I	ONGC	1.2
5	RG(East)-CBM-2001/I	ESSAR	2.15-3.0
TOTAL = 8.385 to 9.00 TCF			

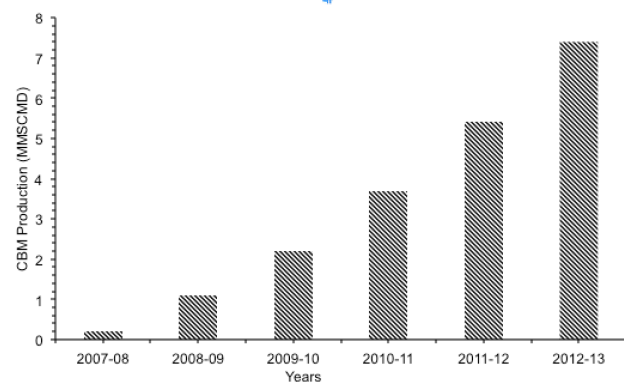


Fig. 1. CBM Production in India [21]

2. Coal Bed Methane

1. Methane is stored in micro pores/cleat as free gas (cleat structure of coal)
2. Methane is found dissolved in water and stored within coal matrix
3. Methane is found adsorbed on the surface of coal and coal matrix

2.1 Calculation of methane volume in coal seam

Pophare, 2008 [36] observed that most of the gas in coal is adsorbed on the internal surface of micro pores and varies directly with pressure and inversely with temperature. The empirical equations to determine volume of adsorb gas is as follows [37]:

$$V = \left[\frac{100 - M - A}{100} \right] \times \frac{V_w}{V_d} \left[K(P)^N - b \times T \right] \tag{1}$$

Where,
 V = Volume of methane gas adsorbed (cc/g), M = Moisture content (%), A = Ash content (%)

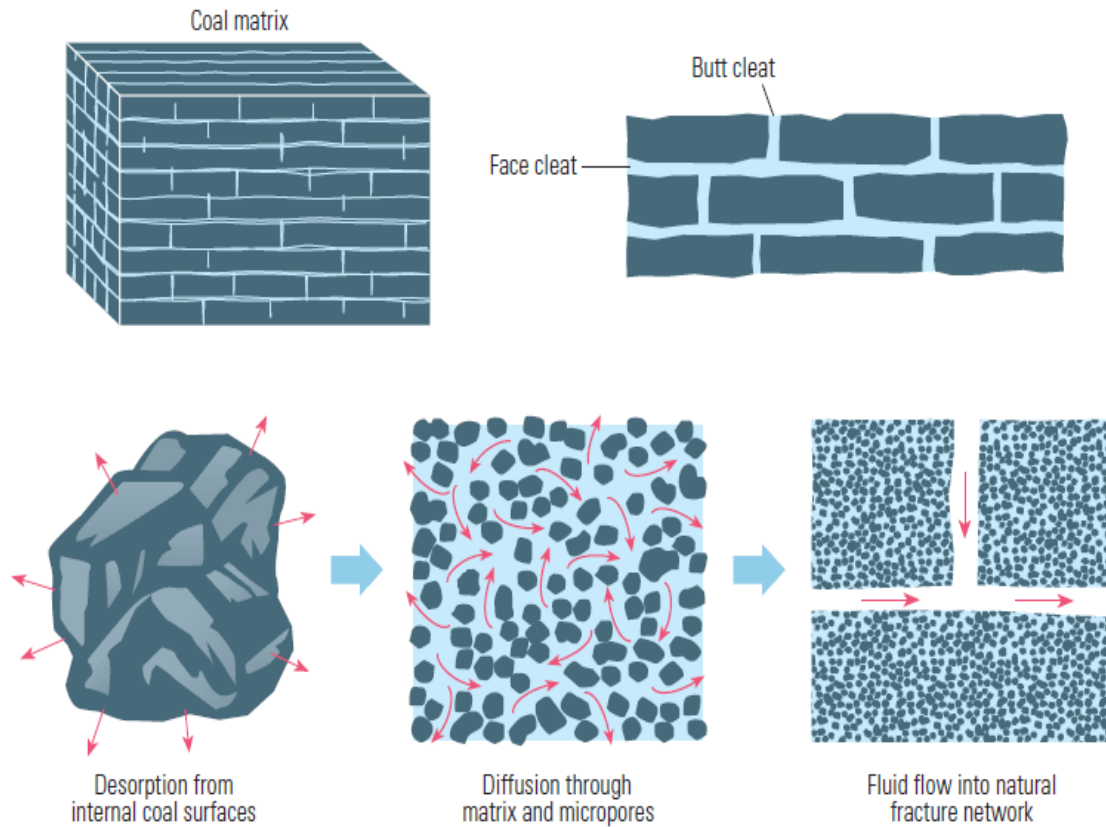


Fig. 2. Cleat structure and migration of methane in coal matrix [25].

Table 3. Reservoir properties of selected coals worldwide [33]

Basin/area	Coal	Age	Rank	Depth, m	No. of seams	Net coal, m	In-situ gas content, cm ³ /g	Perm, md
Sydney	Bulli	Carboniferous–Permian	hi-vol.–lo-vol.	698	1	na	20.8	na
Surat	Walloon	Jurassic	subbit.	150–950	11	na	3.14	500
Qinshui	#3, #15	Carboniferous–Permian	hi-vol. A–metaanth	0–2,500	7–17	0–16	0–36	0.1–4
Cook Inlet/ Susitna	Sterling, Beluga, Tyonek, Chickaloon	Paleocene–Miocene	lig.–anth.	0–1,830	30	0–206	1.1–17	na
San Juan	Fruitland	Cretaceous	subbit.–lo-vol. hi-vol. B–semianth	0–1,300	5	0–21	na	0.1–60
Piceance WCSB	Cameo Mannville	Cretaceous L. Cretaceous	subbit.–lo-vol.	0–3,050	7	18	13–23	0.2
Uinta	Ferron Horseshoe Canyon	U. Cretaceous	hi-vol. C–B	1,500–1,040	3	2–12	7–13	0.1–3
WCSB		U. Cretaceous	subbit. C–A	200–600	6	1–14	3–17	5–20
Powder River	Fort Union	Paleocene	subbit. C–B hi-vol. A–semianth	90–610	2–24	91	2.2	10–1,000
Arkoma	Hartshorne	Pennsylvanian	hi-vol. C–A	85–1,340	3	0.2–2	2.2–18	20–45
Scotland	na	Carboniferous	hi-vol. C–lo-vol.	500–880	10–30	10–24	0.2–6.3	na
England, Northern	na	Carboniferous	hi-vol. C–lo-vol.	710–875	20–30	12–15	3.2–7.5	na
England, Central	E. Pennine	Carboniferous	hi-vol. C–A	430–1,230	25–32	9.1–18	1.5–5.9	na
England, Central	W. Pennine	Carboniferous	hi-vol. A–med. Vol	470–1,100	10–22	7.3–20	0.5–7.1	na
England, Southern	multiple	Carboniferous	med.-vol.–anth.	700–760	10–20	6.1–18	0.4–13	na
Greater Green River	multiple	Cretaceous–Tertiary	subbit.–hi-vol. C	990–1,360	12+	24	1.5–6.9	12.5
Warrior	multiple	Pennsylvanian	hi-vol. A–lo-vol.	60–760	29	13	1.6–17	75
Silesian Basin	multiple	Carboniferous	hi-vol. B–lo-vol.	250–1,750	5+	9	4–9	1–2
Raton	Vermejo	Cretaceous–Paleocene	hi-vol. B–A	75–360	11–20	23	0.8–15	na

Table 4. Reservoir properties of selected coals in India [34]

Gondwana Coal Basin/field					
Coalfields	Ash Content (%)	VM, daf (%)	Vr _o (%)	Vitrinite Maceral Composition (%)	Predicted gas content (cc/gm)
South Karanpura Coalfield	18-25	32-44	0.70 -1.0	50-70	6 -10
Son Valley Coalfields	15-30	33-40	0.76-0.94	57-60	5 - 9
Sohagpur Coalfields			0.65-0.70	40-60	
-III-V Pakaria			0.55-0.65	50-55	
- II-V Churha, Katkona					
- Bottom Seams, working mines					
Mahanadi Valley Coalfields	15-35	32-41	0.60-0.65	40-45	4 - 9
Korba Coalfield	15-40	35-45	0.65-0.55	35-45	2 -7.5
Talchir					
PranhitaGodavari Coalfields					
Wardha Coalfields	07-Nov	35-45	0.55-0.60	25-35	2-7
Pench-Kanhan Valley Coalfields	15-30	32-40	0.50-0.60	45-60	5 - 9
Satpura Basin					
Coal of Barakar Formation					
North-East India	May-20	42-58	0.55-0.70	80-90	0-4
- Tertiary Coals of Assam					

Table 5. Changes in coal properties as Rank increases [35]

Coalification Stage	Moisture (%)	Volatile Matter (%)	Carbon Content (%)	Calorific Value (kcal/kg)	Oxygen Content (%)
	As received	Dry Ash Free	Dry Ash Free	As received	Dry Ash Free
Peat	~75	69 - 63	<60	3500.00	>23
Lignite	35 - 55	63 - 53	65 - 70	4,000 - 4,200	0.23
Sub-bituminous C	30 - 38	53 - 50	70 - 72	4,200 - 4,600	0.20
Sub-bituminous B	25 - 30	50 - 46	72 - 74	4,600 - 5,000	0.18
Sub-bituminous A	18 - 25	46 - 42	74 - 76	5,000 - 5,500	0.16
High Volatile Bituminous C	12-18	46 - 42	76 - 78	5,500 5,900	0.12
High Volatile Bituminous B	10 -12	42 - 38	78 - 80	5,900 - 6,300	0.10
High Volatile Bituminous A	8 - 10	38 - 31	80 - 82	6,300 - 7,000	0.08
Medium Volatile Bituminous	8 - 10	31 - 22	82 - 86	7,000 - 8,000	0.04
Low Volatile	8 - 10	22 - 14	86 - 90	8,000 - 8,600	0.03
Semi-Anthracite	8 - 10	14 - 8	0.90	7,800 8,000	0.04
Anthracite	7 - 9	8 -3	0.92	7,600 - 7,800	0.05
Meta-Anthracite	7 - 9	8 - 3	>92	7600.00	0.05

T = Temperature at given depth, T₀ = ground temperature, h = depth (m), and P = pressure (atm.).

$$\frac{V_w}{V_d} = \left[\frac{1}{0.25 \times M \times 1} \right] \quad (2)$$

Where,

V_w = Volume of gas adsorbed on wet coal (cc/g) and V_d = Volume of gas adsorbed on dry coal (cc/g)

$$K = 0.8 \left(\frac{FC}{VM} \right) + 5.6 \quad (3)$$

Where, FC = Fixed carbon (%), VM = Volatile matter (%), N = Constant, depends on the composition of coal (for most bituminous coals N = 0.39-0.013 × K) and b = Adsorption constant due to temperature change (cc/g^{1/c})

$$T = 2.5 \times \frac{h}{100} + T_0 \quad (4)$$

Where,

The empirical formula for the estimation of methane gas (V_{CH₄}) in coal bed on dry ash free basis is as follows:

$$V_{CH_4} = -325.6 \times \log \left(\frac{VM(daf)}{37.8} \right) \quad (5)$$

Where,

V_{CH₄} = Volume of methane (cc/g), VM (daf) = volatile matter (%) (dry and ash free basis)

3. Transportation of gases in Coal Seam

The intricate and heterogeneous nature of the coal matrix makes the gas storage and transport processes quite complex. Diffusion of gases in macro pores of cleat structure in coal matrix actually responsible for the flow of gas in coal seam. The mechanism of diffusions is molecular diffusion,

Knudsen diffusion and surface diffusion. Out of three mechanisms molecular diffusion preferred when the pore diameter is greater than ten times the mean free path, while Knudsen diffusion may be assumed when the mean free path exceed greater than ten times the pore diameter [38]. The transport process of gas in a coal seam can be expressed as follows [39-41]:

3.1 Darcy’s velocity equation

$$\frac{\varphi_{\beta} \partial S_{e_{\beta}}}{\partial t} + \nabla \cdot \left\{ \frac{K_{\beta}}{\mu_{\beta}} \nabla (p_{\beta} + \rho_{\beta} g H) \right\} = S_{\beta} \tag{6}$$

Where,

β = Phase index, φ_{β} = Porosity, K_{β} = Permeability, μ_{β} = Viscosity, S_e = Saturation, H = Vertical elevation and S_{β} = Represent source terms.

In the above representation, the two components and phases are considered. CO₂ was considered as non-wetting phase while water as a wetting phase. The Darcy's velocity equation for non-wetting and wetting are represented as follows:

Gas phase

$$\frac{\varphi_g \partial S_{e_g}}{\partial t} + \nabla \cdot \left\{ \frac{-K_{abs} \cdot K_{r,g}}{\mu_g} \nabla (p_g + \rho_g g H) \right\} = S_g \tag{7}$$

Water phase

$$\frac{\varphi_w \partial S_{e_w}}{\partial t} + \nabla \cdot \left\{ \frac{-K_{abs} \cdot K_{r,w}}{\mu_w} \nabla (p_w + \rho_w g H) \right\} = S_w \tag{8}$$

Where,

φ = Initial porosity, S_e = Effective saturation, K_{abs} = Absolute permeability of porous medium, $K_{r, \alpha}$ = Relative permeability, μ = Dynamic viscosity, S = source terms, P = Pressure, ρ = Fluid density and g = acceleration due to gravity.

The capillary pressure P_c and the change between the effective saturation and capillary pressure can be calculated as follows:

$$P_c = P_g - P_w \tag{9}$$

$$\gamma_{p,w} = -\gamma_{p,g} = \frac{\varphi_{\alpha} \partial S_{e_{\alpha}}}{\partial p_c} \tag{10}$$

Where,

γ = specific capacity for phases.

It is very important to understand the dynamics of gas flow in coal matrix for successful coal bed methane production. The exploration of gas flow through porous media was started in the petroleum industry for the development of natural gas reservoirs. Schematic of flow of gas through cleat system is shown in (Figure 3 and 4). The elaborative study of gas flow behaviour as well as geo mechanical properties is one of the standard techniques for

estimation of gas permeability and other reservoir parameters. Due to the large variation of pressure in deep reservoir it is not possible to apply ideal gas law in production of CBM in deep pressurized condition. Gas flows behaviour differs in porous media than liquid flow due to its compressibility as well as Klinkenberg effect. Some recent laboratory investigation concluded that the Klinkenberg effect is important in the low permeability formations studied and cannot be ignored [42, 43]. According to Klinkenberg (1941), effective gas permeability at a finite pressure is given as:

$$k_g = k_{\infty} \left(1 + \frac{b}{P} \right) \tag{11}$$

Where, k_{∞} = Absolute gas-phase permeability under very large gas-phase pressure at which condition the Klinkenberg effects are negligible, b = Klinkenberg factor, dependent on the pore structure of the medium and temperature for a given gas, P = gas pressure (Pa)

It was found that ‘b’ generally decreases with increasing permeability

$$b \propto k_{\infty}^{-0.36} \tag{12}$$

Study was also carried out to determine flow characteristics by Knudsen through glass capillaries and found Knudsen flows (independent of pressure) in the fine pore system of coals and Poiseuille flows (proportional to pressure) have been through the larger pores [44]. Triple-porosity/dual-permeability and the coupling effects of effective stress and micro-pore swelling/shrinkage geomechanical deformation approach was studied and found that both the effective stress as well as micro-pore shrinkage effect significantly influence the CBM production performance [45]. Espinoza et al., 2011 [46] observed that the physical properties of gas such as density, viscosity, interfacial tension and bulk compressibility vary with pressure and temperature conditions. Yi et al., 2013 [47] reported that transport property of coal porous media with fractal pore structures is controlled by the maximum pores, the pore size distribution, and the fractal dimension number of pore structure.

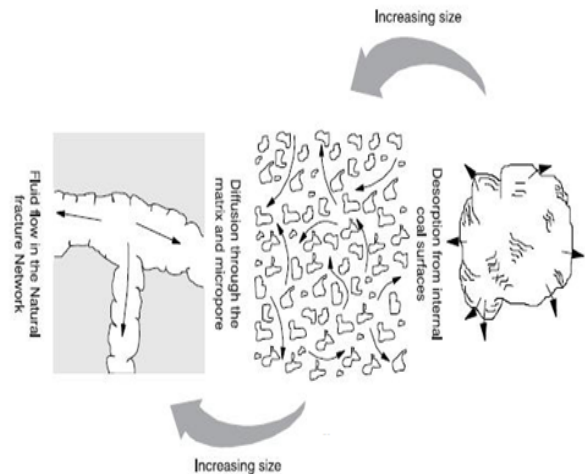


Fig. 3. Schematic of flow of gas through cleat system [48, 49]

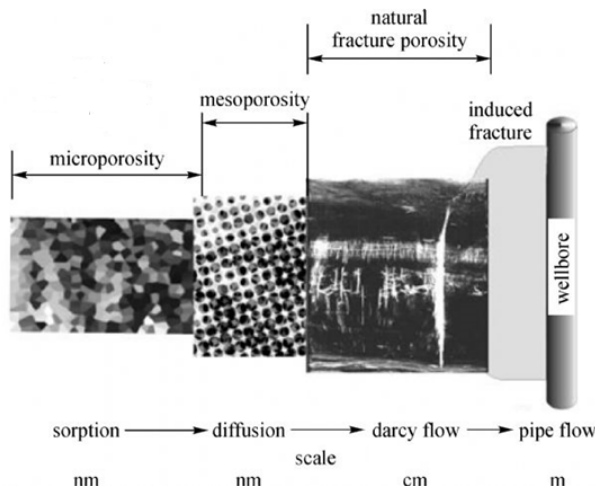


Fig. 4. Multi-scale gases transport in coalbed [50]

4. Coal Matrix

Coal is a typical dual porosity/permeability system containing porous matrix surrounded by fractures and cleat network (Figure 5). The matrix is characterized as solid grains, micro pores (<0.01 μm), and interconnected meso pores (0.01–0.1 μm), while the cleat network includes macro pores (>0.1 μm) and fractures [51, 52]. Harpalani et al., 2010 [53] observed that the volumetric changes in the matrix can be owned to two effects: the pressure-induced effect that is characterized by the coal matrix compressibility and the desorption-induced effect that is characterized by the matrix shrinkage coefficient (ϵ_g). In coal bed methane recovery, gas desorbs from the inner wall surface of coal matrix and transport through pore system to the natural fracture at different gas concentration, and ultimately flow to production line due to pressure difference, hence gas diffusivity in the coal matrix and gas permeability in the cleat is the parameters controlling the rate of flow of gases in coal bed [54, 55]. Pan et al., 2010 [56] observed three different diffusion mechanisms in porous media:

- i. Fickian diffusion where inter-molecular collisions between gas molecules is the dominant mechanism and is significant for large pore sizes and/or high system pressures
- ii. Knudsen diffusion by collisions between the gas molecules and pore walls is important when the mean free path of the gas molecules is greater than the pore size
- iii. Surface diffusion where adsorbed molecular species move along the pore wall surface is important for micro pores with strongly adsorbed species

All these diffusion mechanisms play important roles in gas diffusion in coal matrix. The complexity of the pore system in the coal matrix and the gas-coal interaction was studied by Pan et al., and Li et al., 2010 [56, 57] and observed the sorption rate appears to be one step in anthracite coal sample, however, it was two steps in a crushed sub-bituminous coal sample. The transport of gas in porous media depends on the sizes of pores. With variation of sizes the gas diffusion also varies. As the pore size decrease, gas diffusion type changes from bulk diffusion to

Knudsen diffusion, including the transition region [58, 59]. Mingyue et al., 2014 [60] found the equation for flux at different gas concentration in fractures and diffusion of gas from coal matrix to fractures as:

$$q = D\sigma V_m (c_m - c_f) \tag{13}$$

Where, q = diffusion flux (g/s), D = diffusion coefficient (cm^2/s), σ = shape factor (cm^{-2}), V_m = volume of coal matrix (mL), C_m = mass concentration of gas in coal matrix (g/mL) and c_f = mass concentration of gas in fractures (g/mL). Based on the ideal gas state equation, the gas density in pores of coal matrix is:

$$c_m = \frac{M}{RT} p_m \tag{14}$$

Where, p_m = gas pressure in pores of coal matrix (Pa), M is molar mass of gas (methane, 16g/mol), R = gas constant (8.314510 J/(mol·K)) and T = gas temperature (K).

The gaseous gas density in fractures is:

$$c_f = \frac{M}{RT} p_f \tag{15}$$

Where, p_f = gas pressure in fractures (MPa).

It is very tedious to determine diffusion coefficient and shape factor of coal matrix, while adsorption time τ is commonly used to represent the diffusion ability [61]. The adsorption time is the time when 63.2% of gas content is desorbed, and is in reciprocal relationship with the product of diffusion coefficient and shape factor as:

$$\tau = \frac{1}{D\sigma} \tag{16}$$

The shorter the adsorption time is, the better the diffusion ability as:

$$q = \frac{MV_m}{\tau RT} (p_m - p_f) \tag{17}$$

Coal gas in coal matrix containing free gas and adsorbed gas, the amount of free gas can be calculated through ideal gas state equation, and the amount of adsorbed gas can be obtained by the Langmuir isotherm equation. The average gas density in coal matrix would be [60]:

$$\begin{aligned} \bar{c}_m &= \frac{Q_{\text{adsorption}} + Q_{\text{free}}}{V_m} = \frac{\left(\frac{abp_m}{1+bp_m} + \frac{\phi_m p_m}{\rho p_0} \right) \cdot \rho V_m \cdot M}{V_M \cdot V_m} = \\ &= \left(\frac{abp_m}{1+bp_m} + \frac{\phi_m p_m}{\rho p_0} \right) \cdot \frac{\rho M}{V_M} \end{aligned} \tag{18}$$

Where, \bar{c}_m = average gas density in coal matrix (g/mL), $Q_{\text{adsorption}}$ and Q_{free} = the amount of free gas and adsorbed gas (g) respectively, ϕ_m = porosity of coal matrix (%), a = the maximum adsorption capacity of coal (mL/g), b = adsorption constant (MPa^{-1}), ρ = bulk density of coal mass

(g/mL) and p_0 = standard atmospheric pressure (101.325 kPa).

The mass conservation equation of coal gas in coal matrix is:

$$q = -\frac{\partial c_m V_m}{\partial t} \quad (19)$$

Fractures and coal matrix exchange coal gas, and when the porosity is constant, the mass conservation equation of coal gas in fractures is:

$$\varphi_f \frac{\partial(p_f)}{\partial t} - \frac{K}{\mu} \nabla \cdot (p_f \cdot \nabla p_f) - \frac{1}{\tau} \cdot (1 - \varphi_f)(p_m - p_f) = 0 \quad (20)$$

Where, ϕ_f = fracture porosity (%) and μ = gas dynamic viscosity (1.08×10^{-5} Pa.s for methane).

Combining above equations (15), (16) and (17), the gas pressure of coal matrix changes with time as:

$$\frac{\partial p_m}{\partial t} = -\frac{\frac{1}{\tau} \cdot (p_m - p_f) \frac{M}{RT}}{\left(\frac{ab}{1 + bp_m} - \frac{ab^2 p_m}{(1 + bp_m)^2} + \frac{\varphi_m}{\rho p_0} \right) \frac{\rho M}{V_m}} \quad (21)$$

Equations (18) and (19) are the governing equations for gas diffusion and flow in coal seam.

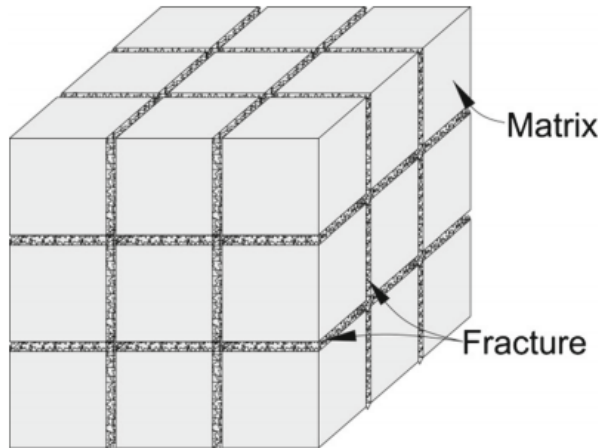


Fig. 5. Dual porosity model of coal [62]

Matrix properties control the swelling transition from local swelling to macro swelling and also control the evolution of coal permeability. Liu et. al., 2011 [63] observed the relation between coal swelling and permeability and concluded that, when the swelling is localized, coal permeability is controlled by the internal fracture boundary condition and behaves volumetrically but when the swelling becomes macro-swelling, coal permeability is controlled by the external boundary condition and behaves non-volumetrically. Chunguang et al., 2014 [64] determined the coal swelling by injecting CO₂ gas in intact coal sample. When CO₂ was injected at 1.72 MPa pressure the volume of coal first swelled and then maintained unchanged, but when injected at 4 MPa the coal volume greatly swelled and then followed a slight recovery. Based on the experimental results it was concluded that the coal deformation is controlled by the competition between adsorption-induced swelling and compression/recovery

determined by the effective stress. Staib et al., 2014 [65] determined the coal swelling with variation of different gases. The different rate of swelling was observed with different gases. Swelling was found slower with CH₄ as comparison to that of CO₂ at the same pressures. Perera and Ranjith, 2012 [66] investigated the coal swelling based on the gas properties and observed that CO₂ has more ability to swell coal than CH₄. Masoudian et al., 2013 [67] studied the flow behaviour of gas in coal seam and found research gap and suggested that, the magnitude and sign of the volume change during coal swelling and their relation with properties of the coal need further investigation. Matrix swelling and shrinkage of coals is an important factor in evaluating CBM reservoirs. However, this phenomenon is not yet fully described for a variety of gasses as well as mixture of different gasses [68].

5. Permeability in Coal Bed

The ease with which fluid flow through cleat structure, fissures as well as pores of coal and coal matrix is termed as permeability. The coal seams are extremely heterogeneous reservoirs whose permeability depend not only on geological age, coal rank, and purity, but also on gas and water saturations, in-situ stresses, and sorbed gas content. The Laboratory-measured permeability anisotropies were reported a 2:1 contrast in face and butt cleats and a 100:1 contrast between face cleat and vertical permeability [69]. The same 2:1 ratio of face cleat to butt cleat permeabilities was also observed in an interference test in San Juan coals [70]. Horizontal permeability anisotropy of 17:1 was reported from an interference test in the Warrior Basin on the basis of soft type curve matches [71]. In all these observation the permeability of face cleat was always higher than that of the butt cleat, attributed the easy flow of gas through the face cleat and but cleat connects the network of flow in gas production. Results also found horizontal permeability larger than vertical permeability by a factor of 42 through simulation of coal well performance in the Great Divide (Greater Green River) Basin [72]. The permeability in coal bed is found in order of microdarcies or nanodarcies, while coal cleat permeabilities ranged from 0.1 to 1,000 md [73]. The higher permeability in coal cleat structure was found as comparison of coal matrix. The range of coal seam permeability differs place to place as well as the types of coal. The gas permeability of high rank coal is different than that of the low rank coal. The gas permeability generally decreases with rank of coal. The permeability of two different coal seams at different locations also differs based on the cleat structure as well as natural fractures in coal. Chatterjee et al., 2010 [74] studied the permeability behaviour of different coal samples obtained from many locations of Jharia coal field, India. The variation in permeability for all coal samples were observed from 0.1 md to 3.5 md. The permeability was also correlated with vertical stress and observed an exponential correlation between them [74]. Coal matrix and cleat permeability governs fluid flow through a coal seam. Reiss et al., 1980 [75] had proposed the match stick model for correlation between permeability and cleat structure. (Figure 6).

Porosity of a coal can be expressed as:

$$\varphi = \frac{2b}{a} \quad (22)$$

Where, ϕ = cleat porosity, b = cleat width and a = cleat spacing.

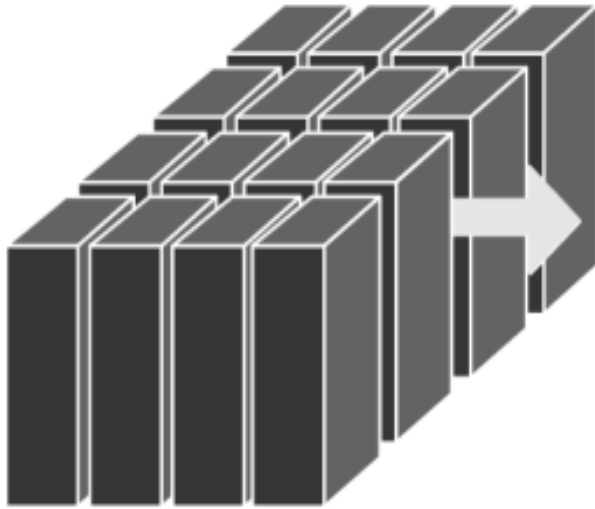


Fig. 6. Matchstick geometry (Reiss et. al., 1980)

Flow down through cleat can be described by Poiseuille's equation

$$q = n \cdot \frac{b^3 l}{12\mu} \cdot \frac{\Delta p}{L} \quad (23)$$

Where, q = flow rate, l = bedding plane height, μ = fluid viscosity, $\Delta p/L$ = pressure gradient and n = Number of cleat.

Total flow down the cleat can also be described by Darcy's law:

$$q = \frac{Ak}{\mu} \cdot \frac{\Delta p}{L} \quad (24)$$

Where, A = flow area, and k = fracture permeability. Fracture permeability can be calculated as:

$$k = \frac{nb^3 l}{12A} \quad (25)$$

Flow area is given by:

$$A = n(a+b)l \quad (26)$$

The relation between permeability and porosity can be plotted as (Figure 7):

Assuming a stiff coal matrix, cleat spacing remains constant as stress changes leads to the following relation for porosity and permeability ratio:

$$\frac{k}{k_i} = \left(\frac{\phi}{\phi_i} \right)^3 \quad (27)$$

It was found that the permeability of coal to methane increases with decreasing gas pressure, in spite of increased effective stress (Harpalani et al., 1990) (Figure 8 and 9).

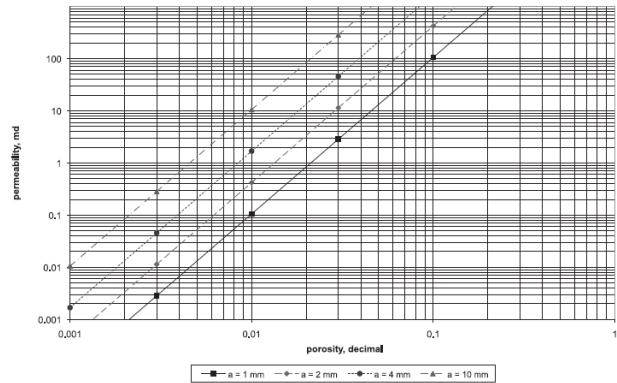


Fig. 7. Cleat permeability as a function of cleat porosity and spacing (Seidle, 2011).

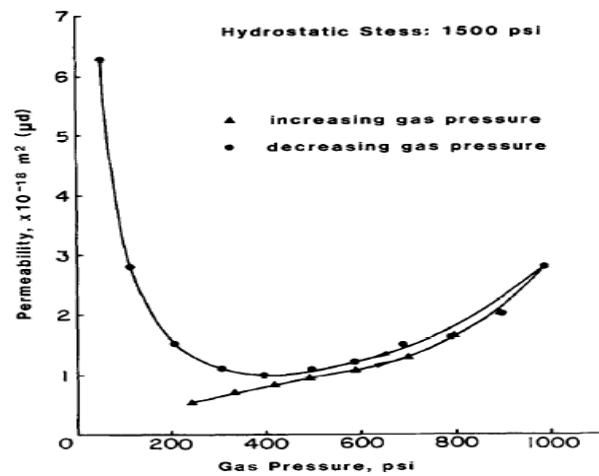


Fig. 8. Variation in permeability of coal to methane for one cycle of increasing and decreasing gas pressure (sample from the Piceance basin) (Harpalani et.al., 1990)

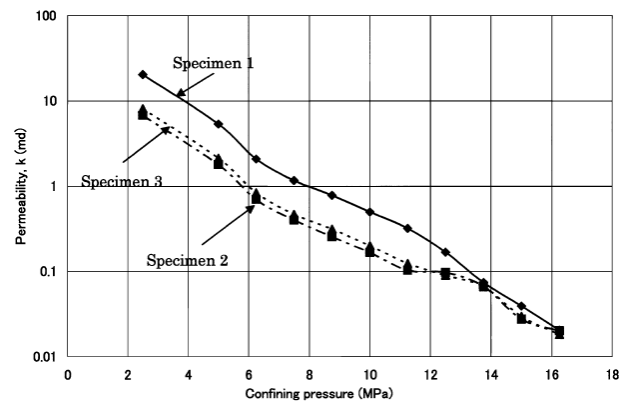


Fig. 9. Effect of confining stress on gas permeability (Li et. al., 2004).

The permeability was found decreased significantly with the increase in confining pressure (Fig 9). The higher confining pressure appears to close internal fractures caused a reduction in permeability [76]. The response of coal containing multiple interacting flaws for a fully cracked medium was investigated experimentally and observed that the presence of bridges across fractures is a crucial component for change in the sense of permeability evolution with pressure [77]. The pore pressure plays an important role in variation of permeability in coal seam. Liu et al., 2012 [78] found the increased permeability with an increases in pore pressure. The permeability was found to increase

continuously with decrease in pore pressure from 7.6 MPa to ~0.35 MPa. The rate of increase is not uniform, with very little increase between 7.6 MPa and 3.5 MPa, which becomes truly significant only below 3.5 MPa [79]. The moisture content and other proximate parameters also affect the ease of flow of gas in coal seam. Pan et al., 2010 [80] observed that matrix permeability decreases by more than 73% for CO₂ and 88% for CH₄ but it decreases 82% from dry coal to wet coal for both CH₄ and CO₂. Perera et al., 2012 [81] investigated the variation of CO₂ permeability in coal at variable pressure and temperature. They observed the significant increase in coal mass permeability with increasing temperature at high CO₂ injection pressure (>10 MPa) and is negligible at low CO₂ injection pressure conditions (<9 MPa). Moore, 2012 [82] studied on permeability behaviour of coal and concluded that the permeability is the most important attribute controlling gas flow in a coal seam reservoir, and is influenced by depth, stress regime within the basin and also, fundamentally, the organic composition of the coal. Zheng et al., 2012 [83] investigated the correlation between permeability with effective stress and pore pressure and observed significant impact of these parameters on permeability. Permeability decreased dramatically with increasing effective stress at the same pore pressure. Permeability also decreased significantly with increasing pore pressures at the same effective stress. Zhu et al., 2013 [52] studied the effect of adsorption pressure of gas on permeability as well crack propagation of side wall in coal seams. They observed the widening of localized damage in well surface and propagation to the matrix and become global damage with increase in gas adsorption pressure. Guo and Cheng, 2013 [84] investigated the effect of in situ conditions on the permeability and observed that the strata stress, gas pressure, strata temperature and depth of occurrence controls the extent of coal fractures.

6. Geo-mechanical properties

Dual-continuum system i.e. porous coal matrix and cleat structure is important characteristic of Coal seams. The geo-mechanical properties and in situ stress conditions of coal reservoir affect the ease of flow of gas through matrix as well as natural fracture. The study of mechanical properties of coal not only reveals the strength but also establish the correlation between permeability and mechanical parameters of coal. Permeability is the multiphase flow processes in coal matrix showed considerable effect on coal bed methane recovery processes [85]. As the stress changes it affect the cleat structure which results in permeability change in coal matrix. Stress value increases with increase in depth that cause decrease in permeability of coal matrix. The permeability and stress is exponentially related to each other as [86]:

$$\frac{k}{k_i} = e^{[-3C_f(\sigma_h - \sigma_{hi})]} \tag{28}$$

Where, k = permeability, k_i = initial permeability, c_f = cleat compressibility, σ_h = hydrostatic stress, and σ_{hi} = initial hydrostatic stress.

At the equal vertical and hydrostatic stress the permeability variation with depth can be expressed as:

$$\frac{k}{k_i} = e^{[-3C_f(\sigma_v - \sigma_{vi})]} \tag{29}$$

However in-situ coal seam remains confined laterally therefore uniaxial strain regime is closer to the mathematical evaluation. Assuming the permeability behaviour only depends on the horizontal stress of the cleat the equation of uniaxial strain can be written as:

$$\epsilon_1 = \frac{1}{E}(\sigma_1 - \nu(\sigma_2 + \sigma_3)) \tag{30}$$

Where, ε = strain, E = Young’s modulus, σ = stress, and ν = Poisson’s ratio.

Mean stress can be written as:

$$\sigma_m = \frac{\sigma_v}{3} \left(\frac{1+\nu}{1-\nu} \right) \tag{31}$$

The expression for the transformation of laboratory result to the in-situ regime condition can be written as:

$$\frac{k}{k_i} = e^{[-C_f \left(\frac{1+\nu}{1-\nu} \right) (\sigma_v - \sigma_{vi})]} \tag{32}$$

Where, σ_v = S – p; S = overburden load, and p = Pore pressure

From above expression the relation between permeability to the depth of the coal seam can be written as:

$$\frac{k}{k_i} = e^{[-C_f \left(\frac{1+\nu}{1-\nu} \right) \cdot A(d-d_i)]} \tag{33}$$

Where, d = Depth and A = constant

Permeability as a function of depth is plotted in (Figure 10).

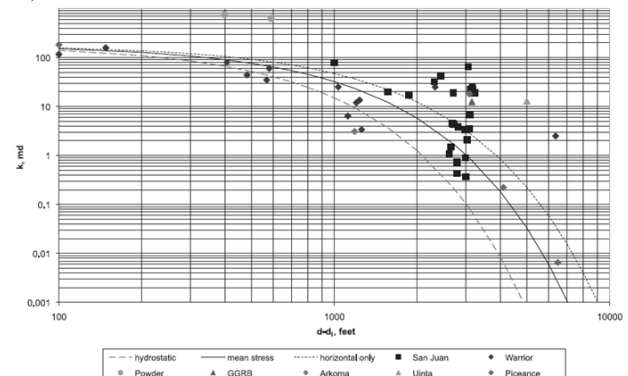


Fig. 10. Coal permeability Vs Depth [33]

As the methane desorbed from the coal matrix the reservoir pressure starts to decrease and at the same time stress value increases cause narrowing of cleat width that results in decline of coal matrix permeability. The change in stress can be related to pore pressure as:

$$\sigma_v - \sigma_{vi} = p_i - p \quad (34)$$

Therefore the change in permeability can be related to the pore pressure as:

$$\frac{k}{k_i} = e^{\left[-C_f \left(\frac{1+\nu}{1-\nu}\right) (p_i - p)\right]} \quad (35)$$

Denis et al., 2010 [87] investigated the strain developed in coal seam during the injection of CO₂ at variable pressure and observed that in confined coal the three-dimensional local strain distribution contributes to both local compression and dilation in spatial directions. Mazumder and Farajzadeh, 2010 [88] developed mechanistic model to determine the correlation between mechanical properties as well as permeability of coal at in situ conditions. They observed that the permeability is highly stress dependent, which declines exponentially with the increase in the confining stress as a result of compaction. Paul and Chatterjee, 2011 [89] investigated the effect of overburden pressure on permeability of Indian coal and observed decreased permeability with increase in vertical stress/sediment overburden load. They established correlation between vertical load and coal permeability and observed second order polynomial with regression coefficient of 0.65. It was observed that increase of confining pressure causes a reduction in pore size as well as permeability, and the flow tends to be dominated more by laminar flow [90]. Study found that increasing confining pressure from 6 MPa to 12 MPa reduces the permeability by a factor of 11 for CH₄, and 28 for CO₂. It also leads to decline in the amount of gas adsorbed by 66% for CH₄ and 59% for CO₂, and thus reduces the swelling strain for each gas [91]. Perera and Ranjith, 2012 [66] observed that the reduction of unconfined compressive strength (UCS) and the elastic modulus of coal caused by super-critical CO₂ adsorption (up to 9 MPa saturation pressure) are much greater compared with the sub-critical CO₂ adsorption in coal because of the greater adsorption potential and dissolution ability of super-critical CO₂ in coal. Tao et al., 2012 [92] observed a significant decrease in permeability and gas production rate in a CBM production well with a fast pressure drop/ high dewatering rate. Chen et al., 2012 [93] studied the effect of geo-mechanical properties and permeability of coal samples and concluded the following:

- When coal swelling parameters remain unchanged, coal permeability profiles are regulated by the initial effective stress.
- Coal permeability reduces initially, recovers and then reaches the final equilibrium magnitude.
- When the confining stress is higher, the final equilibrium coal permeability is much lower than the initial permeability.
- When confining stress conditions remain unchanged, coal permeability profiles are regulated by coal swelling capacity.
- When the confining stress is kept as constant, both the effective stress effect and the swelling strain effect are defined as a function of gas pressure.

- When the fracture compressibility is higher, the permeability enhancement due to the decrease in effective stress may take over the permeability reduction due to swelling.
- The reduction in coal permeability is larger when the effective stress coefficient is lower because the effective stress increases as the effective stress coefficient decreases.
- The sensitivity factor represents the ratio of fracture aperture strain to swelling strain incremental. When the sensitivity factor is higher, the reduction in coal permeability is more significant.

Yang et al., 2012 [94] studied the effect of stress regime on methane production and observed that the effective horizontal stress plays an important role in production of CBM, and the permeability decreases gradually along with the decrease of effective horizontal stress. When the pressure is less than the desorption pressure, the permeability increases caused by the shrinkage of coal matrix, resulted in the increase of CBM output. CBM reservoirs exhibit an extra strain caused by desorption and adsorption. The concept of shrinkage/swelling strain–stress plays an important role in deformation of coal with continued gas production from coal reservoirs [95]. Espinoza et al., 2013 [96] studied the sorption behaviour and mechanical properties of coal and concluded that the knowledge of adsorptive and mechanical properties is critical for calculating coal bed gas reserves and storage capacity, and enabling predictable exploitability. Results showed that gas desorption weakens coal through two mechanisms: (1) reducing the effective stress controlled by the ratio of gas desorption rate over the drainage rate, and (2) crushing coal due to the internal gas energy release controlled by gas composition, pressure and content [97]. Aziz et al., 2013 [98] carried out the permeability testing with the multi-function outburst research rig (MFORR) showed that coal permeability decreases with increasing gas pressure. At higher gas pressures, coal permeability stays stable and changes little with changes in under differing operating range vertical stress conditions of the MFORR. Test clearly demonstrates the coal sample underwent negative volumetric changes or shrinkage with increased confinement pressures axially and laterally. The degree of the volumetric changes was found to be dependent on the level of the applied axial and lateral pressures or stresses. Guo and Cheng, 2013 [54] observed that the effect of the sorption deformation on porosity (permeability) firstly increased rapidly and then slowly with the increase of depth. However, the effect of thermal expansion and effective stress compression on porosity (permeability) increased linearly with the increase of depth. Bo et al., 2014 [29] studied the relationship between permeability and effective stress and observed the nonlinear decreasing representation of permeability with increasing effective stress. Under constant confining stress conditions, the internal swelling ratio can be treated as constant. While under varying confining stress conditions, the internal swelling ratio is a variant. Wang et al., 2014 [99] Zang et al., 2015 [100] have studied the swelling of coal sample with varying stress conditions and concluded as:

- The confining stress, the coal structure, the cleat aperture and the micro lithotypes of coal may

affect the internal swelling, and the mechanism needs to be identified.

- For gaseous and supercritical CH₄ and gaseous CO₂, both the internal swelling and the internal swelling ratio decreased with increasing confining stress under constant pore pressure conditions. Under constant effective stress conditions, the internal swelling increased with increasing pore pressure for both CH₄ and CO₂.
- The internal swelling ratio varied nonlinearly i.e. it decreased at low pore pressures and then ascended as pore pressure increased.
- The internal swelling may be affected by pore pressure, confining stress, sorbate type, coal structure, and coal lithotypes.
- When injecting supercritical CO₂ into coal beds, the permeability reduction may be much greater. Subsequently, the injection efficiency may be much lower compared with the gaseous CO₂ injection.
- The in situ internal swelling ratio could be assumed to be a constant during CBM recovery when the confining stress is greater than 5 MPa.

Espinoza et al., 2014 [101] investigated the effect of triaxial stress conditions on coal fractures and permeability and observed as:

- Fractured coal has a significant non-linear elastic behaviour
- Fractured coal cores show mechanical anisotropy
- Swelling strains, swelling stresses and total uptake are affected by the response of the macro porous and microporous systems and
- Permeability is four times more sensitive to radial (lateral) stress than to axial (vertical) stress.

Harpalani and Mitra, 2010 [53] studied the effect of overburden pressure on coal fracture mechanism and observed the fractures development and increased permeability at CO₂ injection due to depth of the coal and associated overburden stress. They found easily and very early failure of coal sample when CO₂ displaced methane under uniaxial strain conditions. Pan and Connell, 2012 [102] studied the swelling and geo-mechanical behaviour of coal and observed that there are many effects for CBM production and CO₂ sequestration that are poorly understood such as anisotropy in swelling and geomechanical properties, which have only recently been considered but more work is required, further work is required in order to improve the understanding of the reservoir behaviour and coal permeability. More efforts are required to understand the effect of CO₂ adsorption on mechanical properties of coal.

7. Conclusion

The reviews have been focused on CBM fundamentals, permeability as well as geomechanical behaviour of coal matrix that actually affect CO₂/CH₄ adsorption/desorption mechanism. However, in this review the following crucial points have been reported:

- Coal bed methane is being explored and extracted commercially in many countries like USA, Australia, Canada, China, India etc. Exploration and developing of CBM and ECBM in India are likely to have commercial gas in the next few years.
- It is very important to understand the flow mechanism in coal bed reservoir for commercial as well as successful design production and injection well.
- Flow behaviour of gases in coal matrix is one of the important attribute that regulates CBM production and CO₂ sequestration. However there are very few researches that deal the flow behaviour of gases in coal matrix. Hence future work requires investigation on flow behaviour of gases in coal matrix.
- Matrix swelling and shrinkage during adsorption/desorption of gases contribute important factor in evaluating CBM reservoirs. However, this phenomenon is not yet fully described for a variety of gasses.
- The effect of matrix swelling and shrinkage on cleat structure, cleat aperture, cleat compressibility etc. is a topic that should be pursued further and investigated in depth.
- Permeability is one of the most important parameter to describe flow behaviour of gases in coal matrix. There are few experiments that describe the effect of geomechanical properties, cleat system, sorption etc. There are also very limited experimental and numerical studies that describe the permeability of gas mixtures in coal matrix.
- Determination of gas permeability in coal bed reservoir at in situ conditions is very important for successful execution of production as well as injection well.
- Geo-mechanical properties and coal permeability are inter-related to each other. The change in mechanical properties affects coal permeability and as a result gas production as well as CO₂ sequestration process.

This is an Open Access article distributed under the terms of the Creative Commons Attribution License



References

1. K. N. Singh, "Coal Bed Methane Potentiality – Case Studies from Umaria, Korba and Ib-alley Coals, Son-Mahanadi Basin", journal geological society of India, 2010 Vol.76, pp.33-39.
2. F. Colosimo, R. Thomas, J. R. Lloyd, K. G. Taylor, C. Boothman, A. D. Smith, "Biogenic methane in shale gas and coal bed methane: a review of current knowledge and gaps", Int. J. Coal Geol., 2016, Vol. 165, pp. 106-120.
3. D. Ritter, D. Vinson, E. Barnhart, D. M. Akob, M. W. Fields, A. B. Cunningham, "Enhanced microbial coalbed methane generation: a review of research, commercial activity, and

- remaining challenges”, *Int. J. Coal Geol.*, 2015, Vol. 146, pp. 28-41.
4. B. B. Nyakuma, O. Oladokun, A. Jauro, D. D. Nyakuma, “Evaluating the Energy Recovery Potential of Nigerian Coals under Non-Isothermal Thermogravimetry”, 2017, Vol. 217, pp. 1-7, *IOP Conf. Series: Materials Science and Engineering*.
 5. Saleem Qadir Tunio, Swapan Kumar Bhattacharya, Khalil Rehman Memon, Sonny Irawan, Aung Kyaw, Mohd. Faisal Abdullah, “Investigating Methane Adsorption Potential of Malaysian Coal for Coal Bed Methane (CBM) Study”, *Mediterranean Journal of Social Sciences*, 2014, Vol. 5, pp. 178-183.
 6. Pengwei Zhang, Liming Hu, Jay N. Meegoda, Shengyan Gao, “Micro/Nano-pore Network Analysis of Gas Flow in Shale Matrix”, 2015, DOI: 10.1038/srep13501.
 7. Yongbin Zhang, Bin Gong, Junchao Li and Hangyu Li, “Discrete Fracture Modeling of 3D Heterogeneous Enhanced Coalbed Methane Recovery with Prismatic Meshing”, *Energies*, 2015, Vol. 8, pp. 6153-6176.
 8. H. Xu, D. Tang, J. Zhao, S. Li, S. Tao, “A new laboratory method for accurate measurement of the methane diffusion coefficient and its influencing factors in the coal matrix”, *Fuel*, 2015, Vol. 158, pp.239-247.
 9. D. V. Antonov, T. R. Valiullin, R. I. Iegorov, P. A. Strizhak, “Effect of macroscopic porosity onto the ignition of the waste-derived fuel droplets”, *Energy*, 2017, Vol. 119, pp.1152-1158.
 10. R. Yang, S. He, Q. Hu, D. Hu, S. Zhang, J. Yi, “Pore characterization and methane sorption capacity of over-mature organic-rich Wufeng and Longmaxi shales in the southeast Sichuan Basin, China”, *Marine and Petroleum Geology*, 2016, Vol. 77, pp.247-261.
 11. Bogusz and M. Bukowska, “Specific Energy of Hard Coal under Load”, *Studia Geotechnica et Mechanica*, 2015, Vol. 37, pp. 9-16.
 12. Z. Weishauptova, O. Pribyl, I. Sykorova, V. Machovic, “Effect of bituminous coal properties on carbon dioxide and methane high pressure sorption”, *Fuel*, 2015, Vol. 139, pp. 115-124.
 13. T. A. Moore, “Coalbed methane: A review”, *International Journal of Coal geology*, 2012, Vol. 101, pp. 36-81.
 14. Y. Wang, S. Liu and D. Elsworth, “Laboratory investigations of gas flow behaviors in tight anthracite and evaluation of different pulse-decay methods on permeability estimation”, *International Journal of Coal Geology*, 2015, Vol. 149, pp. 118-128.
 15. Md. I. Ismail and D. K. Gupta, “Reservoir Simulation to Diagnose the Causes of Reduced Well Production Efficiency in Coal Bed Methane”, 2015, *Journal of Earth Science & Climatic Change*, Vol. 6, pp. 1-8.
 16. L. Zhang, D. Li, L. Wang and D. Lu, “Simulation of Gas Transport in Tight/Shale Gas Reservoirs by a Multicomponent Model Based on PEBI Grid”, *Journal of Chemistry*, 2015, ID 572434, pp. 1-9.
 17. G. Feast, K. Wu, J. Walton, Z. Cheng, B. Chen, “Modeling and Simulation of Natural Gas Production from Unconventional Shale Reservoirs”, *International Journal of Clean Coal and Energy*, 2015, Vol. 4, pp. 23-32.
 18. C. Guo, M. Wei and H. Liu, “Modeling of Gas Production from Shale Reservoirs Considering Multiple Transport Mechanisms”, *PLoS One*, 2015, Vol. 10, pp. 1-24.
 19. Y. Zhang, B. Gong, J. Li and H. Li, “Discrete Fracture Modeling of 3D Heterogeneous Enhanced Coalbed Methane Recovery with Prismatic Meshing”, *Energies*, 2015, Vol. 8, pp. 6153-6176.
 20. Chandra, “Presentation on Conventional Oil & Gas, CBM and Shale Gas/Oil Opportunities and Shale Gas/Oil Opportunities in India”, Singapore, 2012, 24th-25th, September.
 21. Directorate General of Hydrocarbons (DGH), Ministry of Petroleum & Natural Gas through Government of India, 2009, <http://www.dghindia.org>.
 22. J. Zhang, M. B. Clennell, D. N. Dewhurst, K. Liu, “Combined Monte Carlo and molecular dynamics simulation of methane adsorption on dry and moist coal”, *Fuel*, 2014, Vol. 122, pp. 186-197.
 23. Q. Li, Y. Ju, Y. Bao, Z. Yan, X. Li, and Y. Sun, “Composition, Origin, and Distribution of Coalbed Methane in the Huaibei Coalfield, China”, *Energy Fuels*, 2015, Vol. 29, pp. 546-555.
 24. S. Li and B. Zhang, “Research of Coalbed Methane Development Well-Type Optimization Method Based on Unit Technical Cost”, *Sustainability*, 2016, Vol. 8, pp. 843.
 25. Al-Jubori, S. Johnston, C. B. Stephen, W. Lambert, O. A. Bustos, J. C. Pashin, Y. Wray, “Coalbed Methane: Clean Energy for the World”, 2009, *Oilfield Review Summer*.
 26. P. K. Mukherjee, D. P. Sinha and D. S. Rawat, “Coal Bed Methane: How India fits as a potential candidate in CBM prospect and potentiality”, *SAAEG*, 1999, pp.79- 87.
 27. K. N. Singh, “Coal Bed Methane Potentiality – Case Studies from Umaria, Korba and Ib-Valley Coals, Son-Mahanadi Basin”, *Journal Geological Society of India*, 2010, Vol. 76, pp. 33-39.
 28. R. Chatterjee and S. Paul, “Classification of coal seams for coal bed methane exploitation in central part of Jharia coalfield, India – A statistical approach”, *Fuel*, 2013, Vol. 111, pp. 20-29.
 29. L. Bo, W. Jianping, W. Kai, L. P. Wang, “A method of determining the permeability coefficient of coal seam based on the permeability of loaded coal”, *International Journal of Mining Science and Technology*, 2014, Vol. 24, pp. 637-641.
 30. Junlong Zhao, Dazhen Tang, Hao Xu, Yumin Lv, Shu Tao, “High production indexes and the key factors in coalbed methane production: A case in the Hancheng block, southeastern Ordos Basin, China”, *Journal of Petroleum Science and Engineering*, 2015, Vol. 130, pp. 55-67.
 31. W. Bo, J. Bo, F. Xu, X. Kong, G. Li, X. Wang, W. Chen, M. Geng, “Accumulation of coal-bed gas in the Wangying-Liujia area of the Fuxin basin”, *International Journal of Mining Science and Technology*, 2012, Vol. 22, pp. 1-6.
 32. L. Dawei, J. Chen, Z. Li, G. Zheng, C. Song, H. Liu, Y. Meng and D. Wang, “Controlling Factors, Accumulation Model and Target Zone Prediction of the Coal-bed Methane in the Huanghebei Coalfield, North China”, *Resource Geology*, 2014, Vol. 64, pp. 332-345, pp. 1-9.
 33. John Seidle, “Fundamental of coal bed methane reservoir engineering”, 2011, *Penn Well Corporation, Oklahoma*.
 34. Oil and Natural Gas Corporation Limited (ONGC), Annual Report, <http://www.ongcindia.com>, 2005.
 35. Coal Marketing International Ltd (CMI), 2012-14, <http://www.coalmarketinginfo.com>.
 36. M Pophare, Vinod A Mendhe and A Varade, “Evaluation of coal bed methane potential of coal seams of Sawang Colliery, Jharkhand, India”, *J. Earth Syst. Sci.*, 2008, Vol. 117, pp 121-132.
 37. Kim G A, “Estimating methane content of bituminous coal beds from adsorption data”, *U.S. Bureau of Mines RI8245*, 1977, pp 1-22.
 38. B. Yang, Y. Kang, L. You, X. Li, Q. Chen, “Measurement of the surface diffusion coefficient for adsorbed gas in the fine mesopores and micropores of shale organic matter”, *Fuel*, 2016, Vol. 181, pp 793-804.
 39. G. Liu and A. Smirnov, “Numerical modelling of CO₂ sequestration in un- mineable coal seams”, In *Twenty-Third Annual International Pittsburgh Coal Conference*, 2006, pp 801-817, Pittsburgh, PA.
 40. X. G. Zhang, P. G. Ranjith, M. S. A. Perera, A. S. Ranathunga, and A. Haque, “Gas Transportation and Enhanced Coalbed Methane Recovery Processes in Deep Coal Seams: A Review”, *Energy Fuels*, 2016, Vol. 30, pp 8832-8849.
 41. Z. Li, Z. Hui, G. Hao, “A case study of gas drainage to low permeability coal seam”, *International Journal of Mining Science and Technology*, 2017, Vol. 27, pp 687-692.
 42. D. Yang, W. Wang, W. Chen, S. Wang, and X. Wang, “Experimental investigation on the coupled effect of effective stress and gas slippage on the permeability of shale”, *Sci. Rep.*, 2017, Vol. 7, 44696; doi: 10.1038/srep44696.
 43. R. Sander, Z. P. Luke, D. Connell, “Laboratory measurement of low permeability unconventional gas reservoir rocks: A review of experimental methods”, *Journal of Natural Gas Science and Engineering*, 2017, Vol. 37, pp. 248-279.
 44. F. S. Karn, R. A. Friedel, A. G. Sharkey Jr, “Mechanism of gas flow through coal”, *FUEL*, 1975, Vol. 54, pp. 279-282.
 45. Z. Wei and D. Zhang, “Coupled fluid-flow and geomechanics for triple-porosity/dual-permeability modelling of coal bed methane recovery”, *International Journal of Rock Mechanics & Mining Sciences*, 2010, Vol. 47, pp. 1242-125.
 46. D. N. Espinoza, S. H. Kim, J. C. Santamarina, “CO₂ Geological Storage – Geotechnical Implications”, *KSCE Journal of Civil Engineering*, 2011, Vol. 15, pp. 707-719.
 47. J. yi, S. Huibo, H. Bin, Z. Yibo and Z. JunLing, “Lattice Boltzmann simulation of fluid flow through coal reservoir’s

- fractal pore structure", *Science China Earth Sciences*, 2013, Vol. 56, pp. 1519-1530.
48. G. Penuela, A. R. Ordonez and A. Bejarano, "Linearization of a Generalized Material Balance Equation for Coal bed Methane Reservoirs", *C.T.F Cienc. Tecnol. Futuro*, 1998, Vol. 4.
 49. Kansas Geological Survey, Integrated Subsurface Carbon Sequestration and Enhanced Coalbed Natural Gas Recovery Using Cement Kiln Emissions, Wilson County, Kansas, KGS Open-file 2006-13.
 50. G. G. X. Wang, X. Zhang, X. Wei, X. Fu, B. Jiang, Y. Qin, "A review on transport of coal seam gas and its impact on coalbed methane recovery", *Front. Chem. Sci. Eng.*, 2011 Vol. 5, pp. 139-161.
 51. Y. Yao and D. Liu, "Effects of igneous intrusions on coal petrology, pore-fracture and coal bed methane characteristics in Hongyang, Handan and Huaibei coalfields, North China", *International Journal of Coal Geology*, 2012 Vol. 96-97, pp. 72-81.
 52. W. C. Zhu, C. H. Wei, J. Liu, T. Xu, D. Elsworth, "Impact of Gas Adsorption Induced Coal Matrix Damage on the Evolution of Coal Permeability", *Rock Mech. Rock Engg.* 2013, Vol. 46, pp. 1353-1366.
 53. S. Harpalani, A. Mitra, "Impact of CO₂ Injection on Flow Behaviour of Coal bed Methane Reservoirs", *Transp. Porous Med.*, 2010, Vol. 82, pp. 141-156.
 54. P. Guo and Y. Cheng, "Permeability Prediction in Deep Coal Seam: A Case Study on the No. 3 Coal Seam of the Southern Qinshui Basin in China", *Scientific World Journal*, 2013, doi: 10.1155/2013/161457.
 55. Y. Lv, Z. Li, D. Tang, H. Xu and X. Chen, "Permeability Variation Models for Unsaturated Coalbed Methane Reservoirs, Oil & Gas Science and Technology", 2016 Vol. 71, pp. 1-14.
 56. Z. Pan, L. D. Connell, M. Camilleri, "Effects of matrix moisture on gas diffusion and flow in coal", *Fuel*, 2010, Vol. 89, pp 3207-3217.
 57. D. Li, Q. Liu, P. Weniger, Y. Gensterblum, A. Busch, B. M. Krooss, "High-Pressure sorption isotherms and sorption kinetics of CH₄ and CO₂ on coals", *Fuel*, 2010, Vol. 89, pp 569-80.
 58. B. Nie, Z. Li, W. Ma, "Diffusion micro mechanism of coal bed methane in coal pores", *Coal Geology & Exploration*, 2000, Vol. 28, pp 20-22.
 59. X. He and B. Nie, "Diffusion Mechanism of Porous Gases in Coal Seams", *Journal of China University of Mining and Technology*, 2001, VOL. 30, pp. 1-4.
 60. W. Mingyue and W. Jiren, "The Effect of Gas Diffusion in Coal Matrix on Gas Migration in Coal Seams of Various Permeability", *EJGE*, 2014, Vol. 19, pp 6693-6703.
 61. H. Tiancai and Q. Yong, "Technology of exploration, development and utilization of coal bed methane. Xuzhou, China", 2007, China University of Mining and Technology Press.
 62. J. E. Warren, and P. J. Root, "The behaviour of natural fractured reservoirs", *Soc. Pet. Eng. J.*, 1963, Vol. 3, pp. 245-255.
 63. J. Liu, J. Wang, Z. Chen, S. Wang, D. Elsworth, Y. Jiang, "Impact of transition from local swelling to macro swelling on the evolution of coal permeability", *International Journal of Coal Geology*, Vol. 88, pp. 31-40, 2011.
 64. W. Chunguang, W. M. Zhu, G. Bin, T. Yuling, "Deformation transition of intact coal induced by gas injection", *International Journal of Mining Science and Technology*, Vol. 24, pp. 833-838.
 65. G. Staib, R. Sakurovs, E. MacA Gray, "Kinetics of coal swelling in gases: Influence of gas pressure, gas type and coal type", *International Journal of Coal Geology*, 2014, Vol. 132, pp. 117-122, 2014.
 66. M. S. A. Perera and P. G. Ranjith, "Carbon dioxide sequestration effects on coal's hydro-mechanical properties: a review", *Int. J. Energy Res.*, 2012, Vol. 36, pp. 1015-1031.
 67. M. S. Masoudiana, D. W. Aireya and A. El-Zein, "Mechanical and flow behaviours and their interactions in coal bed geo sequestration of CO₂", *Geomechanics and Geoengineering: An International Journal*, 2013, Vol. 8, pp. 229-243.
 68. L. J. Pekot and S. R. Reeves, "Modelling the Effects of Matrix Shrinkage and Differential Swelling on Coal bed Methane Recovery and Carbon Sequestration", paper 0328, 2003, Proceedings of the Coal bed Methane Symposium, Tuscaloosa.
 69. B. W. Gash, R. F. Volz, G. Potter, J. M. Corgan, "The effects of cleat orientation and confining pressure on cleat porosity, permeability and relative permeability in coal", in Proceedings of the International Coal bed Methane Symposium, 1993 Tuscaloosa, University of Alabama,
 70. M. J. Mavor and J. R. Robinson, "Analysis of Coal Gas Reservoir Interference and Cavity Well Tests", Paper SPE 25860., 1993, Presented at the Joint Rocky Mountain Regional and Low Permeability Reservoirs Symposium, Denver, Colorado.
 71. R. A. Koenig and P. B. Stubbs, "Interference Testing of a Coal bed Methane Reservoir", 1986, Presented at the SPE Unconventional Gas Technology Symposium, Louisville, Kentucky.
 72. G. B. C. Young, J. E. McElhiney, R. Dhir, M. J. Mavor and I. K. A. Anboub, "Coal bed Methane Production Potential of the Rock Springs Formation, Great Divide Basin, Sweetwater County, Wyoming", 1991, Presented at the SPE Gas Technology Symposium, Houston, Texas.
 73. G. J. Bell and K. C. Rakop, "Hysteresis of methane/coal sorption isotherms", 61st Annual Technical Conference and Exhibition of the Society of Petroleum Engineers, 1986, New Orleans.
 74. R. Chatterjee, S. Paul, P. K. Pal, V. K. Srivastava, "Formation Evaluation and Characterization of CBM Reservoir Rocks from Well logs of Jharia Coalfield, India", *Petrotech*, 2010, New Delhi, India.
 75. L. H. Reiss, C. R. B. McKee, "Stress-dependent permeability and porosity of coal and other geologic formations", *Society of Petroleum Engineers Formation Evaluation*, 1980, Vol. 3, p.p 81.
 76. H. Siriwardane, I. Haljasmaa, R. McLendon, G. Irdi, Y. Soong, G. Bromh, "Influence of carbon dioxide on coal permeability determined by pressure transient methods", *International Journal of Coal Geology*, 2009, Vol. 77, pp. 109-118.
 77. G. Izadi, S. Wang, D. Elsworth, J. Liu, Y. Wu, D. Pone, "Permeability evolution of fluid-infiltrated coal containing discrete fractures", *International Journal of Coal Geology*, 2011, Vol. 85, pp. 202-211.
 78. Liu, S. and Harpalani, S., "Gas Production Induced Stress and Permeability Variations in Coal bed Methane Reservoirs", *American Rock Mechanics Association, 46th US Rock Mechanics / Geomechanics Symposium*, 2012, Chicago, IL, USA.
 79. Liu S. and Harpalani S., "Gas Production Induced Stress and Permeability Variations in Coal bed Methane Reservoirs", *46th US Rock Mechanics/Geomechanics Symposium*, 2012, Chicago, IL, USA.
 80. Z. Pan, L. D. Connell, M. Camilleri, "Laboratory characterisation of coal reservoir permeability for primary and enhanced coal bed methane recovery", *International Journal of Coal Geology*, 2010, Vol. 82, pp. 252-261.
 81. M. S. A. Perera, P. G. Ranjith, S. K. Choi, D. Airey, "Investigation of temperature effect on permeability of naturally fractured black coal for carbon dioxide movement: An experimental and numerical study", *Fuel*, 2012, Vol. 94, pp. 596-605.
 82. T. A. Moore, "Coalbed methane: A review", *International Journal of Coal Geology*, 2012, Vol. 101, pp 36-81.
 83. G. Zheng, Z. Pan, Z. Chen, S. Tang, L. D. Connell, S. Zhang, B. Wang, "Laboratory study of gas permeability and cleat compressibility for CBM/ECBM in Chinese coals", *Energy Exploration and Exploitation*, 2012, Vol. 30, pp. 451-476.
 84. P. Guo and Y. Cheng, "Permeability Prediction in Deep Coal Seam: A Case Study on the No. 3 Coal Seam of the Southern Qinshui Basin in China", *The Scientific World Journal*, Article, 2013, ID 161457, DOI. 1155/2013/161457.
 85. X. R. Wei, G. X. Wang, P. Massarotto, S. D. Golding, V. Rudolph, "A review on recent advances in the numerical simulation for coal bed-methane-recovery process", *SPE Reserv. Eval. Eng.*, 2007 Vol. 10, pp. 657-666.
 86. L. H. Reiss, "The Reservoir Engineering Aspects of Fractured Reservoirs", 1980, Paris, Gulf Publishing Company.
 87. J. Denis, N. Pone, P. M. Halleck, J. P. Mathews, "3D characterization of coal strains induced by compression, carbon dioxide sorption, and desorption at in-situ stress conditions", *International Journal of Coal Geology*, 2010 Vol. 82, pp. 262-268.
 88. S. Mazumder and F. Farajzadeh, "An alternative mechanistic model for permeability changes of coalbeds during primary recovery of methane", 2010, SPE Asia Pacific Oil and Gas Conference and Exhibition. SPE, Brisbane, Queensland.
 89. S. Paul and R. Chatterjee, "Determination of in-situ stress direction from cleat orientation mapping for coal bed methane

- exploration in south-eastern part of Jharia coal field, India”, International Journal of Coal Geology, 2011, Vol. 87, pp. 87-96.
90. M. S. A. Perera, P. G. Ranjith, S. K. Choi, D. Airey, “Numerical simulation of gas flow through porous sandstone and its experimental validation”, Fuel, 2011 Vol. 90, pp. 547-554.
91. S. Wang, D. Elsworth, J. Liu, “Permeability evolution in fractured coal: The roles of fracture geometry and water-content”, International Journal of Coal Geology, 2011 Vol. 87, pp. 13-25.
92. S. Tao, Y. Wang, D. Tang, H. Xu, Y. Lv, W. He, Y. Li, “Dynamic variation effects of coal permeability during the coal bed methane development process in the Qinshui Basin, China”, International Journal of Coal Geology, 2012 Vol. 93, pp. 16-22.
93. Z. Chena, J. Liua, Z. Panb, L. D. Connellb, D. Elsworth, “Influence of the effective stress coefficient and sorption-induced strain on the evolution of coal permeability: Model development and analysis”, International Journal of Greenhouse Gas Control, 2012 Vol. 8, pp. 101-110.
94. Y. Yanga, X. Penga, X. Liu, “The Stress Sensitivity of Coal Bed Methane Wells and Impact on Production”, International Conference on Advances in Computational Modelling and Simulation, 2012 Vol. 31, pp. 571-579.
95. S. Liu and S. Harpalani, “Determination of the Effective Stress Law for Deformation in Coal bed Methane Reservoirs”, Rock Mech. Rock Engg. 2013 DOI 10.1007/s00603-013-0492-6.
96. D. N. Espinoza, M. Vandamme, P. Dangla, J. M. Pereira and S. Vidal-Gilbert, “A transverse isotropic model for micro porous solids: Application to coal matrix adsorption and swelling”, Journal of Geophysical Research: Solid Earth, 2013 Vol. 118, pp. 6113-6123.
97. S. Wang, D. Elsworth, J. Liu, “Mechanical Behaviour of Methane Infiltrated Coal: the Roles of Gas Desorption, Stress Level and Loading Rate”, Rock Mech. Rock Engg., 2013 Vol. 46, pp. 945-958.
98. N. Aziz, T. Ren, J. Nemicik and L. Zhang, “Permeability and Volumetric Changes in Coal under Different Test Environment”, Acta Geodyn. Geomater., 2013 Vol. 10, pp. 163-171.
99. K. Wang, J. Zang, G. Wang, A. Zhou, “Anisotropic permeability evolution of coal with effective stress variation and gas sorption: Model development and analysis”, International Journal of Coal Geology, 2014 Vol. 130, pp. 53-65.
100. J. Zang, K. Wang, Y. Zhao, “Evaluation of gas sorption-induced internal swelling in coal”, Fuel, 2015 Vol. 143, pp. 165-172.
101. D. N. Espinoza, M. Vandamme, J. M. Pereira, P. Dangla, S. V. Gilbert, “Measurement and modelling of adsorptive-poromechanical properties of bituminous coal cores exposed to CO₂: Adsorption, swelling strains, swelling stresses and impact on fracture permeability”, International Journal of Coal Geology, 2014 Vol. 134-135, pp. 80-95.

Abbreviation

CBM: Coal bed methane

nm: Nano meter

Gt: Giga ton

BT: billion ton

TCM: trillion cubic meter

TCF: trillion cubic foot

MMSCMD: million std. cubic meter per day

daf: dry ash free basis

atm.: atmosphere pressure

md: milidarcy

VM: Volatile matter

ECBM: Enhanced coal bed methane

µm: Micrometer

SCF: Standard cubic foot

V_L: Langmuir volume constant, SCF/ton

P_L: Langmuir pressure constant, psia

psia: per square inch absolute

µd: microdarcy

psi: per square inch